Impact of a behavior model linearization strategy on the tolerance analysis of over-constrained mechanisms☆

A. Dumas [a,b,*], J.-Y. Dantan [a], N. Gayton [b]

[a] LCFC, Arts et Métiers ParisTech Metz, 4 rue Augustin Fresnel, 57078 METZ CEDEX 3, France
[b] Clermont Université, IFMA, UMR 6602, Institut Pascal, BP 10448, F-63000 Clermont-Ferrand, France

HIGHLIGHTS

- A tolerance analysis approaches overview is proposed.
- A linearization procedure of the behavior model is required for both approaches.
- Some linearization strategies provide conservative probability of failure results.
- A confidence interval is obtained using two different linearization strategies.
- The order of magnitude of the probability has an effect on the convergence speed.

All manufactured products have geometrical variations which may impact their functional behavior. Tolerance analysis aims at analyzing the influence of these variations on product behavior, the goal being to evaluate the quality level of the product during its design stage. Analysis methods must verify whether specified tolerances enable the assembly and functional requirements. This paper first focuses on a literature overview of tolerance analysis methods which need to deal with a linearized model of the mechanical behavior. Secondly, the paper shows that the linearization impacts the computed quality level and thus may mislead the conclusion about the analysis. Different linearization strategies are considered, it is shown on an over-constrained mechanism in 3D that the strategy must be carefully chosen in order to not over-estimate the quality level. Finally, combining several strategies allows to define a confidence interval containing the true quality level.

1. Introduction

Geometrical tolerances influence both design functional performance and production costs, because their effects are felt at all stages of the product life cycle, so these are key elements for the design process. Appropriate design tolerances enable complex mechanical assemblies, made up of several parts, to be assembled and functional at low cost. Moreover, they enable the quality level of assemblies to be increased and ensure a high mechanical reliability of the product. To evaluate whether the design tolerances are relevant to ensure the functionality of the product, a methodology such as tolerance analysis must be applied. The tolerance analysis of mechanisms aims at verifying whether the specified design tolerances allow to reach a given quality level of the product during its design stage. The goal is to avoid the manufacturing of non-functional mechanisms. Hence, tolerance analysis is a key element [1]:

- to improve product quality,
- to reduce manufacturing costs,
- to manage and reduce waste in production.

Tolerance analysis can be divided into two approaches, whose techniques to build the behavior model are different. A comparison of both approaches is proposed in order to show their similarities and differences. Although the formulations of the mathematical models are different, both approaches need to deal with an approximated model coming from a linearization procedure in order to perform the analysis method and compute a predicted quality

level. Indeed, the analysis method is based on mathematical operations which require a linear model: a Minkowski sum and linear optimization problem with constraints. For both approaches, the linearization procedure implies simplifying the behavior model and thus modifying the accuracy of the mathematical model. This operation creates a model error which needs to be quantified. In addition, depending on the type of linearization, the corresponding error created may be different. It appears interesting to determine the best linearization procedure in order to limit the approximation error.

This paper first proposes a brief comparison of tolerance analysis approaches to show why the linearization procedure is required for both techniques. Then the paper intends to show that the linearization procedure has, of course, a real impact on the predicted quality level and on the computer time to obtain the information. However, a carefully chosen linearization procedure strategy enables this impact to be reduced. Indeed, depending on the considered strategy, the quality level may be under-estimated or over-estimated, and the computing time can be greatly increased. The analysis method must therefore take these parameters into account when applying a linearization procedure.

The next section of this paper focuses on a literature overview of both tolerance analysis approaches in order to show that a linearization procedure of the behavior model is required for all approaches. Section 3 presents the considered linearization strategies of the behavior model. The mathematical operation for the linearization of non-linear equations is detailed. Section 4 integrates the mathematical description and the solution of a tolerance analysis problem based on the model proposed by Dantan and Qureshi et al. [2,1]. Section 5 is devoted to an impact analysis of the linearization procedure on an industrial application. Results of the linearization impact are shown and discussed in this section. A conclusion ends the paper.

2. Tolerance analysis overview

Tolerance analysis aims at verifying the value of functional requirements after tolerances have been specified on each component of a mechanism. Three main issues exist [3]:

1. Modeling geometrical deviations due to the manufacturing process and modeling gaps between features.
2. Building a mathematical model to simulate the behavior of the mechanism, taking into account deviations and gaps.
3. Developing analysis methods to estimate the quality level.

2.1. Geometrical models

Modeling geometrical deviations and gaps are required in order to perform items 2 and 3. Both deviation and gap characterize a displacement between two surfaces of a mechanism. The geometry of the mechanism parts can be modeled in different ways:

- nominal surface: ideal surface whose dimensions and positions match the design.
- skin model: real manufactured surface.
- substitute surface: perfect surface associated with the skin model where the form defects are neglected.

In the present paper the form defects are omitted, so the representation of the geometrical deviations and the gaps is based on substitute surfaces. It could be between two substitute surfaces or between a substitute surface and a nominal surface [2]. Geometrical deviations (situation or/and intrinsic deviations) are modeled by random variables, written $\mathbf{X} = \{X_1, \ldots, X_n\}$. Gaps are modeled by free variables, written $\mathbf{G} = \{g_1, g_2, \ldots, g_m\}$, which need to be computed by the analysis method. Small displacements and kinematic displacements may be considered; they are used either to model small mobilities of the mechanism due to deviations and gaps, or kinematic displacements in joints.

Several representations are mentioned in the literature to deal with displacements. They can be expressed using one of the following techniques: kinematic formulation [4,5], small displacement torsor (SDT) [6,7], matrix representation [8], vectorial tolerancing [9]. The analysis method formulation is based on the small displacement torsors, see Section 4, but it is not limited to one of these techniques; all representations are suitable.

2.2. Behavior models

Building a behavior model allows to know how features of a mechanism interact, that is why relations characterizing its behavior have to be identified. In particular, these relations concern dimensional chains, in order to link features in contact with each other, with or without gaps. In addition, other relations have to be considered to prevent features from penetrating into others when there are gaps. Tolerance analysis can be divided into two distinct categories: displacement accumulation and tolerance accumulation [1]. The first category defines constraints on parameters [2,1] and the second one defines admissible volumes of variations [10–13].

- The goal of displacement accumulation is to model the influences of the deviations on the geometrical behavior of the mechanism. The relation uses the following form [14]:

$$Y = f(\mathbf{X}, \mathbf{G}) \tag{1}$$

  where Y is the response of the system (a characteristic such as a gap or a functional characteristic). The function f represents the deviation accumulation of the mechanism; it can be an explicit analytical expression, an implicit analytical expression or a numerical simulation. The difficulty in determining the function f increases with the complexity of the studied system [15,2,16].
- The aim of tolerance accumulation is to simulate the composition of tolerances i.e. linear tolerance accumulation, 3D accumulation. The admissible deviations are mapped using several vector spaces in a region of hypothetical parametric space. Tolerance accumulation uses relations between all domains to characterize the geometrical behavior. The literature mentions several techniques to represent geometrical tolerances or dimensioning tolerances, among which are T-maps® [10,17,11], gap spaces [18,19] and deviation domains [12,13].

In both cases, several types of domains and constraints are defined. Although the behavior model is based on different mathematical tools, an analogy between these types is possible. Both representations of mechanical behavior have similarities; a brief parallel of both approaches is presented in Table 1.

2.3. Tolerance analysis problem formulations

The tolerance analysis method must define a mathematical formulation able to take into account all the characteristics of the behavior model and to provide an accurate computed quality level. A comparison of the quality level formulations is presented in Table 2.

Different analysis method techniques exist, such as worst-case analysis and statistical analysis [14,2]:

- The goal of statistical tolerance analysis is to compute the probability that the requirement can be satisfied under given individual tolerances [14,24,19].
- The worst case analysis method (also called deterministic or high–low analysis method) involves defining the dimensions and tolerances such that any possible combination of workpieces provides an admissible assembly of the mechanism. In the examination of the functional requirement, the worst possible combination of each deviation is considered [25,26].

Table 1
Comparison of the behavior models between the displacement accumulation approach and the tolerance accumulation approach.

Displacement accumulation	Tolerance accumulation
• **Deviation constraints**: *Probability distributions* Random variables whose distributions and parameter values are known, e.g. $X \sim \mathcal{N}(\mu_X, \sigma_X)$, [1].	• **Deviation volume**: $V_d(\mathbf{X}, \mathbf{G})$ Deviation space (T-Maps® [11,20], deviation domains [20]) representing the admissible variations of a feature within its tolerance zone.
• **Interface constraints**: $C_i(\mathbf{X}, \mathbf{G}) \leq 0$ and $C_{i*}(\mathbf{X}, \mathbf{G}) = 0$ Characterize the non-interference or association between substitute surfaces, which are nominally in contact, by limiting gaps between them [1].	• **Clearance volume**: $V_c(\mathbf{X}, \mathbf{G})$ Hypervolume of admissible variations (i.e. without interference) of a frame with respect to another [20]. Frequency distributions are also used in T-Maps® approach [21].
• **Functional condition**: $C_f(\mathbf{X}, \mathbf{G}) \leq 0$ Limits the orientation and the location between surfaces in relative displacement, which are in functional relation [1].	• **Functional volume**: $V_f(\mathbf{X}, \mathbf{G})$ Specific volume characterizing the admissible variation space of an assembly so as to satisfy the functional requirement [20].
• **Compatibility equations**: $C_c(\mathbf{X}, \mathbf{G}) = 0$ Geometrical behavior of the mechanism expressed by the composition relations of displacements in various topological loops [1].	• **Relation between volumes**: $V_{d1}(\mathbf{X}, \mathbf{G}) \oplus V_{d2}(\mathbf{X}, \mathbf{G}) \ominus V_{c1}(\mathbf{X}, \mathbf{G})$ Minkowski sums or intersections performed according to the different dimensional chains of the mechanism on hypervolumes to obtain accumulated volumes [20].

Table 2
Comparison of tolerance analysis methods between the displacement accumulation approach and the tolerance accumulation approach.

Displacement accumulation	Tolerance accumulation
• **Assembly requirement**: The assembly of a mechanism with gaps must be ensured. The various features, in the presence of deviations, must be assembled without interfering with each other.	
○ "there exists an admissible gaps configuration of the mechanism such that the assembly requirement (interface constraints) and the compatibility equations are respected" [1]. $\exists \mathbf{G} \in \mathbb{R}^m : C_c(\mathbf{X}, \mathbf{G}) = 0 \bigwedge C_i(\mathbf{X}, \mathbf{G}) \leq 0 \bigwedge C_{i*}(\mathbf{X}, \mathbf{G}) = 0$	○ In this case, the assembly requirement is satisfied when the intersection of all accumulated clearance domains is not empty [20]. $\sum V_d(\mathbf{X}, \mathbf{G}) \subset \sum V_c(\mathbf{X}, \mathbf{G})$
• **Functional requirement**: Once the assembly requirement is verified, the influence of the geometrical deviations can be evaluated on a functional characteristic, which is basically a maximum or a minimum clearance on a feature which has an impact on the performance of the mechanism.	
○ "for all admissible gap configurations of the mechanism, the geometrical behavior and the functional requirement are respected" [1]. $\forall \mathbf{G} \in \left\{ \mathbf{G} \in \mathbb{R}^m : C_c(\mathbf{X}, \mathbf{G}) = 0 \bigwedge C_i(\mathbf{X}, \mathbf{G}) \leq 0 \bigwedge C_{i*}(\mathbf{X}, \mathbf{G}) = 0 \right\} : C_f(\mathbf{X}, \mathbf{G}) \geq 0$	○ The functional requirement is satisfied when the accumulated deviation and clearance domain remains within the functional domain [20]. $\sum V_d(\mathbf{X}, \mathbf{G}) \oplus V_c(\mathbf{X}, \mathbf{G}) \subset \sum V_f(\mathbf{X}, \mathbf{G})$
• **Mathematical tools**: For both requirements, an optimization algorithm is required, taking into account all defined constraints. The formulation is detailed in Section 4.1. Cylinder joints result in quadratic interface constraints, making the optimization problem more difficult to solve. A solution is to linearize these constraints.	• **Mathematical tools**: In order to be able to apply Minkowski sums or intersections to compute accumulated hypervolumes, domains have to be linear. A cylinder type joint in a mechanism leads to the definition of a non-linear clearance domain, so it has to be linearized in several facets [22,23].

2.4. Conclusion

Tolerance analysis approaches are based on different techniques to provide the quality level of a designed mechanism. The formulation to check the assembly requirement and the functional requirement are different, and hence the required mathematical tools are also different. However, neither method can deal with a non-linear behavior model, i.e. model with quadratic constraints coming from cylinder joints. For tolerance displacement, the use of an optimization algorithm is required to determine the gap values. Qureshi et al. noticed in [1] that in some cases the result was not admissible, because the given result violates constraints during the resolution. Using numerical simulations, up to 10% of the results were not admissible. It is then not conceivable to perform simulations with such a high loss percentage. A possible solution is to use other types of optimization algorithms, such as genetic or evolutionary algorithms. However, these algorithms are very time-consuming so they cannot be used in numerical simulation such as Monte Carlo simulation. In addition, with a non-linear optimization algorithm, the global minimum may not be found (required for the functional condition) whereas the global minimum is found in linear programming. For tolerance accumulation, in order to compute the accumulated domains, Minkowski sums or the intersection of domains must be applied. These operations require dealing with linear domains to be applied [11,22,23]. Based on these two reasons, we chose to linearize the non-linear equations of the behavior model. The present paper focuses on studying the impact of such a simplification of the behavior model on the computed quality level. This is based on the displacement accumulation approach, but the previous analogy has shown that this study is also relevant for the tolerance accumulation approach. Using the displacement accumulation approach, the quality level corresponds to the probability of failure to be evaluated, one relative to the assembly requirement and one relative to the functional requirement.

3. Linearization procedure for the behavior model

Some interface constraints or deviation domain are written in a quadratic form and they need to be linearized. For instance, computing the distance between two points leads to defining nonlinear

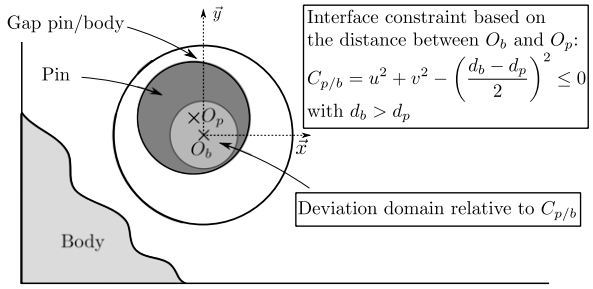

Fig. 1. Admissible area of displacement of the pin center (O_p) with respect to the pin hole center (O_b). The variables u and v correspond respectively with the distance between both points along the x-axis and y-axis and d_b and d_p correspond respectively with the diameter of the pin hole and the pin.

equations. Indeed, the distance between the point A of coordinates (x_A, y_A) and the point B of coordinates (x_B, y_B) is expressed as follows:

$$d(A, B) = \sqrt{(x_A - x_B)^2 + (y_A - y_B)^2}. \tag{2}$$

In order to remove the square root, it is better to deal with the squared distance which provides a quadratic equation. As an example, the displacement of a pin center with respect to the pin hole center is limited in order to prevent the pin from penetrating into the body. Fig. 1 shows the quadratic interface constraint and deviation domain characterizing the limit distance between the pin center and the pin hole center. This distance must not exceed the radius difference.

Let the quadratic function, to be linearized, be written as defined by Eq. (3). The considered strategies are based on a first-order linearization of function C_i to the point P_k of coordinates $(\Delta R \cos\theta_k, \Delta R \sin\theta_k)$, where ΔR is the radius difference and $\theta_k = \frac{2k\pi}{N_d}$, for $k = 1, \ldots, N_d$, is an angle whose parameter N_d enables the number of linearizations to be adjusted.

$$C_i(u, v) = u^2 + v^2 - \Delta R^2. \tag{3}$$

Linearization corresponds to a discretization of the admissible area of displacement, which is a 2D circle, into a polygon whose number of facets depends on N_d. Nevertheless, this operation does not correspond to a discretization of the geometry. It is the quadratic constraint that corresponds to a circle equation that is linearized. Several Linearization strategies are considered: see Fig. 2. Given $C_i(\mathbf{X}, \mathbf{G}) = u^2 + v^2 - \Delta R^2 \leq 0$, an interface constraint, the linearization operation provides new inequalities depending on the type of linearization:

Type 1: linearization following an inner polygon:

$$C_i^{(k)}(\mathbf{X}, \mathbf{G}) = u\cos\theta_k + v\sin\theta_k - \Delta R\cos\frac{\theta_1}{2} \leq 0$$

Type 2: linearization following a medium polygon (average between inner and outer polygons):

$$C_i^{(k)}(\mathbf{X}, \mathbf{G}) = u\cos\theta_k + v\sin\theta_k - \frac{\Delta R}{2}\left(1 + \cos\frac{\theta_1}{2}\right) \leq 0$$

Type 3: linearization following an outer polygon:

$$C_i^{(k)}(\mathbf{X}, \mathbf{G}) = u\cos\theta_k + v\sin\theta_k - \Delta R \leq 0$$

with $\theta_1 = \frac{2\pi}{N_d}$ and $\Delta R > 0$. One interface constraint becomes N_d interface constraints, increasing significantly the number of constraints, but these constraints have the advantage of being linear in displacement.

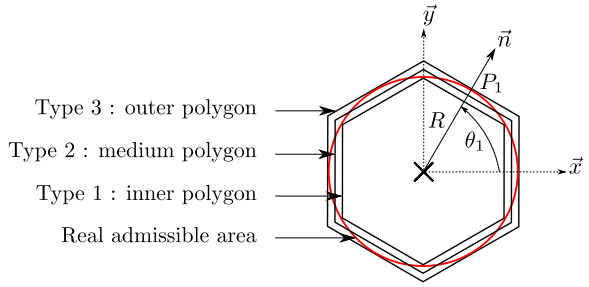

Fig. 2. The 3 types of linearization of the real admissible area of displacement, here with 6 facets.

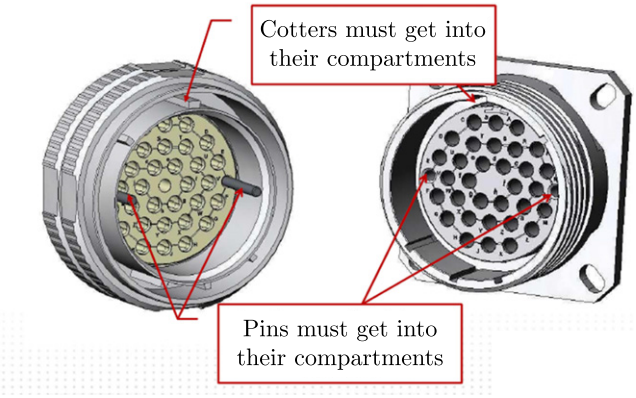

Fig. 3. Electrical connector.

Fig. 3 shows an industrial electrical connector where such a linearization procedure is required. Indeed, the mechanism has two cylinder joints, which will involve writing quadratic constraints.

4. Mathematical formulation and solution method for a tolerance analysis problem

This section presents the formulation of the tolerance analysis problem based on the displacement accumulation approach and the applied solution method to compute the probabilities of failure. This method is first proposed by Qureshi et al. [1].

4.1. Formulation of a tolerance analysis problem

According to Table 1, the behavior model comprises three types of equation: interface constraints, compatibility equations and a functional condition. Assuming **X** is the vector of the geometrical deviations modeled by random variables and **G** the vector of the gaps, let the set of interface constraints be:

$$\left\{C_i^{(j)}(\mathbf{X}, \mathbf{G}) \leq 0\right\}_{j=1,\ldots,N_{C_i}} \tag{4}$$

where N_{C_i} is the number of interface constraints. Let the set of compatibility equations be:

$$\left\{C_c^{(k)}(\mathbf{X}, \mathbf{G}) = 0\right\}_{k=1,\ldots,N_{C_c}} \tag{5}$$

where N_{C_c} is the number of compatibility equations.

It is specified in Table 2 that to check the assembly requirement it is only necessary to find at least one configuration (a specific set of gaps) such that the interface constraints and compatibility equations are satisfied.

The defect probability, P_{fa}, for the assembly requirement is given by the following equation:

$$P_{fa} = 1 - \text{Prob}\left[\exists\tilde{\mathbf{G}} | C_i(\mathbf{X}, \tilde{\mathbf{G}}) \leq 0\right] \tag{6}$$

where $\tilde{\mathbf{G}}$ is a vector of gaps verifying the set of compatibility equations $\left\{C_c^{(k)}(\mathbf{X}, \tilde{\mathbf{G}}) = 0\right\}$ for $k = 1, \ldots, N_{C_c}$. The method to compute this probability is to maximize the sum of gaps with interface constraints; a solution reveals the existence of an admissible configuration of gaps such that all constraints and equations are satisfied, whereas if no solution can be provided, it means that at least one constraint is violated, thus the assembly is not possible because there is at least one interference between two components of the mechanism. The defect probability is given by the equation as follows:

$$P_{fa} = \text{Prob}\left(\begin{array}{c} \nexists \max_{\tilde{\mathbf{G}}} \sum \tilde{\mathbf{G}} \\ \text{with } C_i^{(1)}(\mathbf{X}, \tilde{\mathbf{G}}) \leq 0 \\ \vdots \\ C_i^{(N_{C_i})}(\mathbf{X}, \tilde{\mathbf{G}}) \leq 0 \end{array}\right) \tag{7}$$

where the maximization of the sum of gaps is an artificial function. The goal is only to know if a solution can be found to satisfy all the given constraints.

The functional requirement consists of checking whether a functional characteristic Y respects its assigned threshold Y_{th}. The functional condition $C_f(\mathbf{X}, \mathbf{G}) = Y_{th} - Y(\mathbf{X}, \mathbf{G}) \geq 0$ is defined and must be verified for all admissible gap configurations, see Table 2. However, all configurations do not have to be checked, indeed, in order to compute the defect probability, it is necessary to find at least one admissible configuration where the functional condition is not respected:

$$P_f = \text{Prob}\left[\exists \tilde{\mathbf{G}}_{\text{admissible}} | C_f(\mathbf{X}, \tilde{\mathbf{G}}) \leq 0\right] \tag{8}$$

where $\tilde{\mathbf{G}}_{\text{admissible}}$ are gaps values verifying all interface constraints and compatibility equations. This corresponds with finding the worst gap configuration; this configuration provides the worst value of the functional condition. The technique to find the worst admissible configuration of gaps for the functional condition is to minimize C_f with interface constraints:

$$P_f = \text{Prob}\left(\begin{array}{c} \min_{\tilde{\mathbf{G}}} C_f(\mathbf{X}, \tilde{\mathbf{G}}) \leq 0 \\ \text{with } C_i^{(1)}(\mathbf{X}, \tilde{\mathbf{G}}) \leq 0 \\ \vdots \\ C_i^{(N_{C_i})}(\mathbf{X}, \tilde{\mathbf{G}}) \leq 0 \end{array}\right). \tag{9}$$

4.2. Solution method based on Monte Carlo simulation and optimization

The classic solution method combines a Monte Carlo simulation and an optimization algorithm [1]. As all constraints and functional conditions are linear, an optimization scheme using a simplex technique is chosen to solve both optimization problems defined in Eqs. (7) and (9). The different steps of the solution procedure are described below:

1. A Monte Carlo population is defined: n_{MC} sampling of the random variables, $\mathbf{X}^{(i)}$, $i = 1, \ldots, n_{MC}$.
2. The optimization algorithm is launched for each sample (either maximization of the sum of gaps or minimization of the functional condition).
3. The probabilities of failure are estimated using the following equation:

$$\tilde{P}_{fa,f} = \frac{1}{n_{MC}} \sum_{i=1}^{n_{MC}} I_D(\mathbf{x}^{(i)}) \tag{10}$$

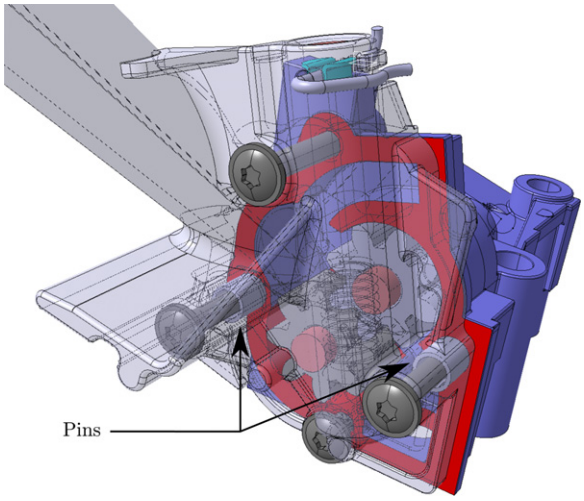

Fig. 4. Gear pump.

where $I_D(\mathbf{X})$ is the indicator function; for the assembly requirement the function is:

$$I_{D_{fa}}(\mathbf{X}) = \begin{cases} 1 & \text{if no solution can be provided} \\ 0 & \text{if a solution is found.} \end{cases} \tag{11}$$

For the functional requirement it is defined as follows:

$$I_{D_f}(\mathbf{X}) = \begin{cases} 1 & \text{if } C_f(\mathbf{X}) \leq 0 \\ 0 & \text{if } C_f(\mathbf{X}) > 0. \end{cases} \tag{12}$$

N.B.: Beaucaire et al. [24] propose a new solution method to deal with overconstrained mechanisms based on a decomposition of the mechanism into several main configurations. Considering these configurations, the probability formulation becomes the probability of an intersection of events, each event being associated to one specific configuration. Due to the linearization procedure, the number of events may increase considerably, which is why this new formulation is not used in the initial phase.

5. Impact of the linearization procedure on an industrial application

The application is based on a gear pump, see Fig. 4, which has two parts positioned with two pins. Fig. 5 shows a half pump view. The joint between the two positioned parts is a planar contact. The positioning of these two parts has an influence on the angle of both gear axes. The functionality of the pump can be reduced if the assembly precision of the parts is insufficient.

Based on this pump, a simplified over-constrained mechanism is studied. Fig. 6 shows the mechanism with amplified gaps between parts. This is a 3D version of the 2D mechanism used to illustrate the linearization procedure in Section 3. Both pins (3) and (4) are fixed to part (2) so as to have only two parts in relative movement. In addition, the planar contact a between (1) and (2) is assumed to be perfect, thus without gaps; only kinematic displacements are possible for this joint. The functional requirement concerns the deviation of point G of part (1) with respect to part (2). This point G can be seen as a functional point representative of one axis of the gear pump.

5.1. Behavior model of the mechanism

The model behavior is briefly described in the following sections. The complete equations are given in Appendix A.

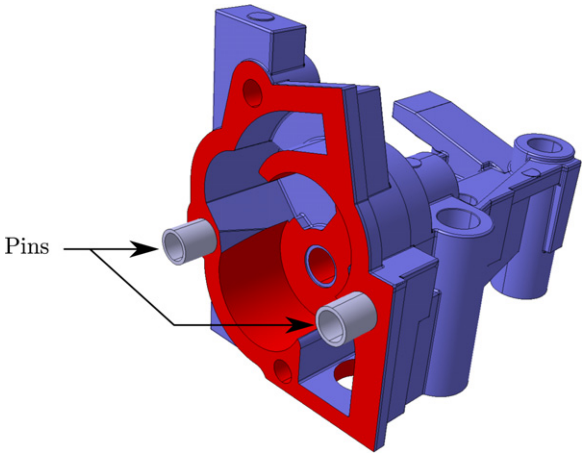

Fig. 5. Half gear pump.

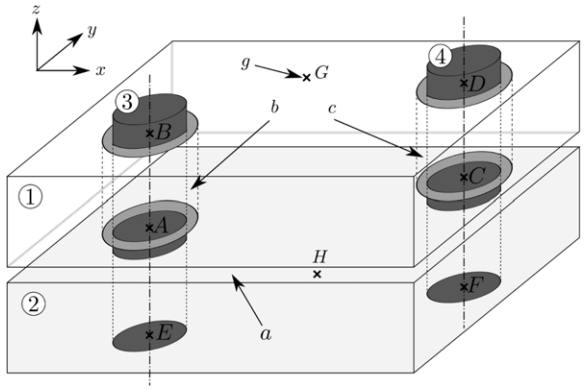

Fig. 6. Mechanism in 3D.

Dimensions between points are deterministic; point A is used as an origin to define the coordinates of the other points. A set of parameters is defined, $\{l_1, \ldots, l_{11}\}$, to model these dimensions.

Fig. 7 shows the joint graph of the mechanism where deviation torsors and clearance torsors are represented. Deviation torsors $T_{ia/i}$ are defined to model the geometrical deviations of a substitute surface ia with respect to the nominal surface i. A torsor is composed of three rotation components a, b and c and three translation components u, v and w. Each torsor depends on the type of surface to model. For example, the deviation torsor of the substitute surface 1b with respect to the nominal surface 1 is defined as follows:

$$\{T_{1b/1}\} = \begin{Bmatrix} a_{1b1} & u_{1b1} \\ b_{1b1} & v_{1b1} \\ 0 & 0 \end{Bmatrix}_A . \tag{13}$$

The other deviation torsors required are $\{T_{2b/2}\}$, $\{T_{1a/1}\}$, $\{T_{2a/2}\}$, $\{T_{1c/1}\}$, $\{T_{2c/2}\}$, $\{T_{1g/1}\}$ and $\{T_{2g/2}\}$. They are defined in Appendix A.1. Moreover, intrinsic deviations are considered: the diameters of the pins and their pin holes: d_{1b}, d_{3b}, d_{1c} and d_{4c}. All these parameters are modeled using random variables with a normal distribution.

Gaps between joints are modeled by clearance torsors: $\{G_{1a/2a}\}$, $\{G_{3b/1b}\}$, $\{G_{4c/1c}\}$ and $\{G_{2g/1g}\}$. According to the assumptions, there are no clearance torsors between pins (3), (4) and their pin holes in part (2): $\{G_{3b/2b}\} = \{G_{4c/2c}\} = \{0\}$. Additionally, the torsor $\{G_{1a/2a}\}$ only represents the kinematic displacement because the joint is assumed to be without gaps. Their form is shown in Appendix A.1. Gaps are the optimization parameters when checking the assembly requirement, see Eq. (7), or finding the worst gap configuration, see Eq. (9).

Fig. 8 shows the top view of the mechanism with amplified deviations and gaps. Only translation components of the deviation torsor and clearance torsor can be represented.

Compatibility equations are written using topological loops of the joint graph, see Fig. 7. There are 5 joints and 4 workpieces (without taking into account the functional joint) so 2 assembly requirement topological loops are studied ($N_{joints} - N_{workpiece} + 1$) which provides 12 linear equations. The loops used are written below:

- Loop (1), (2), (3), expressed in A:

$$\begin{aligned} \{T_{1/1}\}_A &= \{0\} \\ &= \{T_{1/1b}\} + \{G_{1b/3b}\} + \{G_{3b/2b}\} + \{T_{2b/2}\} \\ &\quad + \{T_{2/2a}\} + \{G_{2a/1a}\} + \{T_{1a/1}\} . \end{aligned} \tag{14}$$

- Loop (1), (3), (2), (4), expressed in A:

$$\begin{aligned} \{T_{1/1}\}_A &= \{0\} \\ &= \{T_{1/1b}\} + \{G_{1b/3b}\} + \{G_{3b/2b}\} + \{T_{2b/2}\} \\ &\quad + \{T_{2/2c}\} + \{G_{2c/4c}\} + \{G_{4c/1c}\} + \{T_{1c/1}\} . \end{aligned} \tag{15}$$

Equations obtained with these loops are detailed in Appendix A.2.

The functional condition is written using a topological loop going through the functional condition. The loop (1), (3), (2), C_f expressed in G is taken to obtain a relationship with the functional characteristics $u_{2g/1g}$ and $v_{2g/1g}$:

$$\begin{aligned} \{T_{1/1}\}_G = \{0\} = &\{T_{1/1b}\} + \{G_{1b/3b}\} + \{G_{3b/2b}\} + \{T_{2b/2}\} \\ &+ \{T_{2/2g}\} + \{G_{2g/1g}\} + \{T_{1g/1}\} . \end{aligned} \tag{16}$$

This loop provides two equations with which the functional characteristic can be written; this is the sum of the displacement $u_{2g/1g}$ and $v_{2g/1g}$:

$$\begin{aligned} u_{2g1g} + v_{2g/1g} = &\, u_{1b1} + l_9 b_{1b1} + u_{3b1b} - l_8 C_{3b1b} + l_9 b_{3b1b} \\ &- u_{2b2} - l_9 b_{2b2} + u_{2g2} - u_{1g1} \\ &+ v_{1b1} - l_9 a_{1b1} + v_{3b1b} - l_9 a_{3b1b} \\ &+ l_7 C_{3b1b} - v_{2b2} + l_9 a_{2b2} + v_{2g2} - v_{1g1} . \end{aligned} \tag{17}$$

This characteristic must not exceed a threshold d_{th}; the functional condition is given as follows:

$$C_f(\mathbf{X}, \mathbf{G}) = d_{th} - (u_{2g1g} + v_{2g/1g}) \geq 0. \tag{18}$$

The non-interference conditions must be checked for two joints: surface b between pin (3) and pin hole (1) and surface c between pin (4) and pin hole (1).

- Non-interference 1b/3b:

$$C_i^{(1)} = u_{3b1b}^2 + v_{3b1b}^2 - \left(\frac{d_{1b} - d_{3b}}{2}\right)^2 \leq 0 \tag{19}$$

$$\begin{aligned} C_i^{(2)} &= (u_{3b1b} + l_3 b_{3b1b})^2 + (v_{3b1b} - l_3 a_{3b1b})^2 \\ &\quad - \left(\frac{d_{1b} - d_{3b}}{2}\right)^2 \leq 0. \end{aligned} \tag{20}$$

- Non-interference 1c/4c:

$$C_i^{(3)} = u_{4c1c}^2 + v_{4c1c}^2 - \left(\frac{d_{1c} - d_{4c}}{2}\right)^2 \leq 0 \tag{21}$$

$$\begin{aligned} C_i^{(4)} &= (u_{4c1c} + l_4 b_{4c1c})^2 + (v_{4c1c} - l_4 a_{4c1c})^2 \\ &\quad - \left(\frac{d_{1c} - d_{4c}}{2}\right)^2 \leq 0. \end{aligned} \tag{22}$$

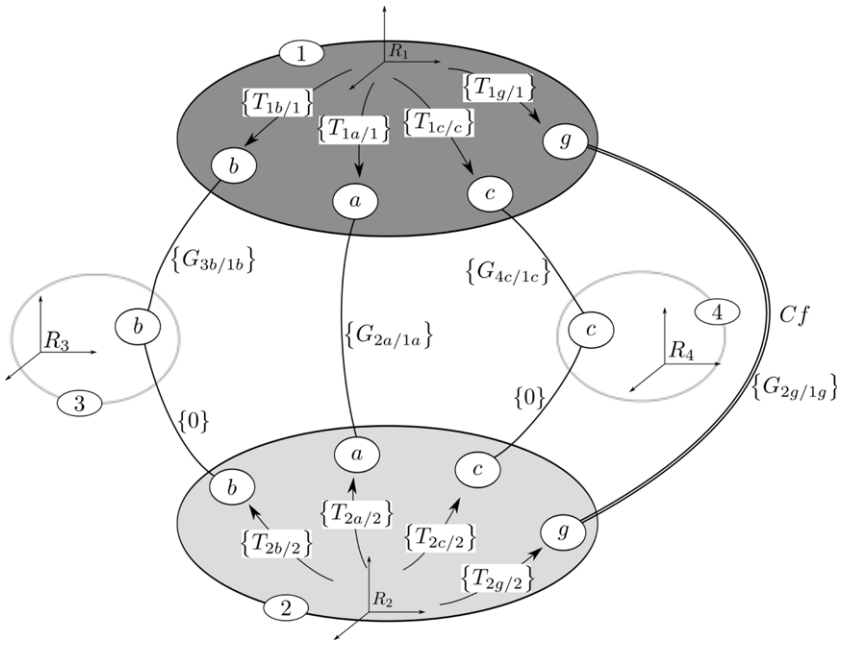

Fig. 7. Joint and deviation graph associated with the studied mechanism in 3D.

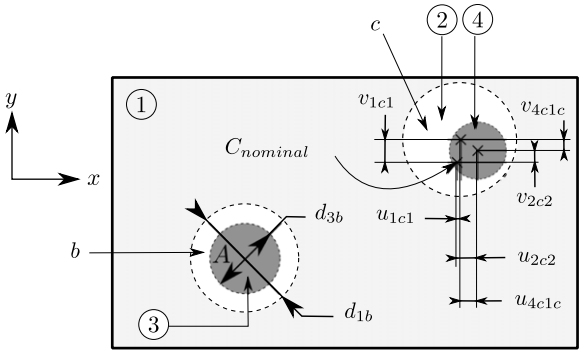

Fig. 8. Top view of the mechanism with amplified deviations and gaps. Intrinsic deviations are represented for pins (3): d_{1b} and d_{3b}. In addition, deviations of surfaces 1c and 2c with respect to their nominal surface are represented: u_{1c1}, v_{1c1}, u_{2c2}, v_{2c2}. Point $C_{nominal}$ corresponds to the case where no deviations are considered. Gaps components for joint 1c/4c are also shown: u_{4c1c} and v_{4c1c}.

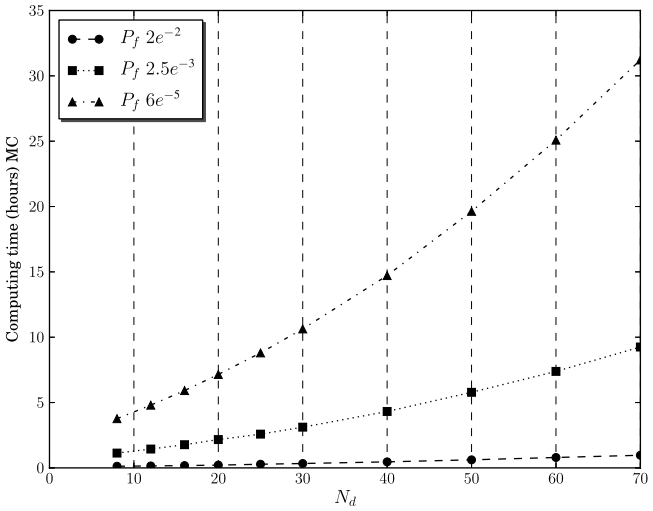

Fig. 9. Evolution of computing time as a function of the number of linearizations and for different orders of magnitude for the probability of failure. Simulation performed with an Intel Core i7-2720.

These four inequalities are linearized following the different strategies proposed in Section 3.

5.2. Numerical results

All parameter values: dimensions, means, standard deviations and probability laws, are necessary for tolerance analysis. Pins diameters and situation deviations are defined as random variables following a normal distribution. Several standard deviation values are set in order to obtain different orders of magnitude of probabilities of failure. Monte Carlo simulations are performed on three different populations. The number of samples n_{MC} is chosen in order to yield a coefficient of variation on the probability of failure (see Eq. (23)) of lower than 5%.

$$\text{C.O.V.}_{P_f} = \sqrt{\frac{1 - P_f}{P_f n_{MC}}}. \tag{23}$$

Fig. 9 shows the variation in computing time for each simulation as a function of the number of linearizations. The required time is naturally longer for a larger number of linearizations because the constraint optimization problem is more complex to solve. Secondly, the order of magnitude of the probability has a strong influence on the computing time; indeed the dash–dot curve with triangle markers represents the smallest target probability and the computing time increases faster than for the others. Therefore, it is very important to select the best linearization strategy in order to obtain an accurate enough result and to avoid useless computing time.

5.2.1. Impact of the number of linearizations on probability of failure convergence

Only results pertaining to probabilities of around 10^{-2} are presented in this section. Other results are shown in the Appendices. Numerical results are given in Table 3; the corresponding curves are shown in Figs. 10 and 11. The results show that the number of

Table 3
Probabilities of failure obtained with the first set of values, order of magnitude 10^{-2}.

	Set of values 1					
	P_{fa} ($\times 10^{-2}$)			P_f($\times 10^{-2}$)		
N_{samples}	3*e*5			3*e*5		
C.O.V.	∼0.7%			∼1.2%		
95% C.I.	∼0.18			∼0.1		
N_d	Inner	Medium	Outer	Inner	Medium	Outer
8	6.72	6.37	6.06	1.15	1.61	2.20
12	6.53	6.37	6.23	1.75	2.01	2.31
16	6.48	6.39	6.31	1.81	1.95	2.11
20	6.42	6.37	6.31	1.90	2.01	2.1
25	6.39	6.35	6.32	1.96	2.01	2.09
30	6.38	6.36	6.34	1.97	2.03	2.08
40	6.37	6.36	6.34	1.98	2.01	2.03
50	6.37	6.36	6.35	2.01	2.02	2.04
60	6.36	6.36	6.35	2.01	2.02	2.03
70	6.36	6.36	6.36	2.02	2.02	2.03

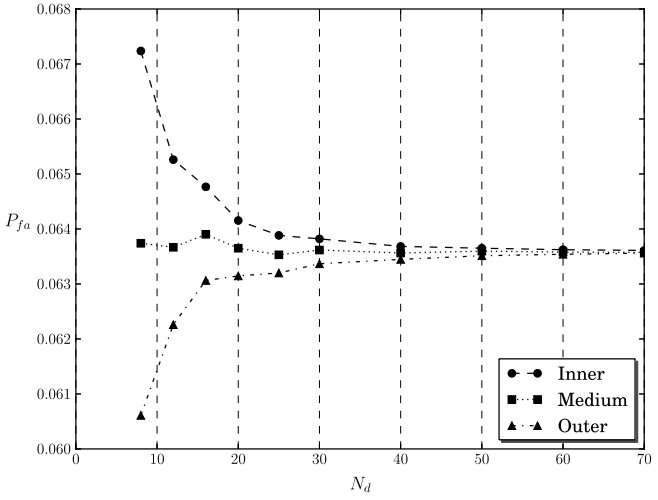

Fig. 10. Convergence of the probability of failure of the assembly requirement for the first set of values.

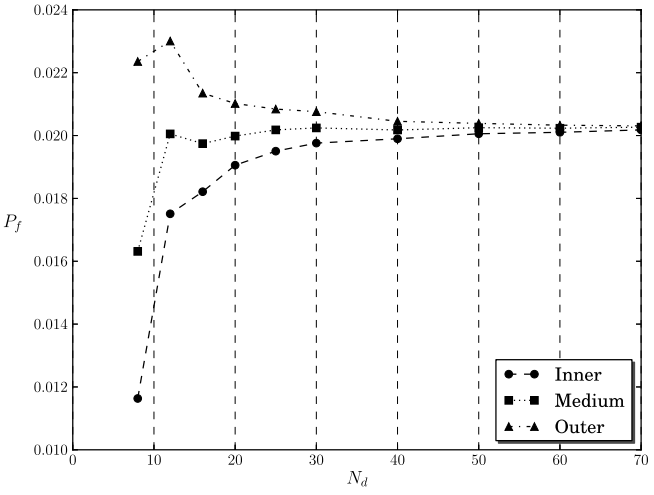

Fig. 11. Convergence of the probability of failure of the functional requirement for the first set of values.

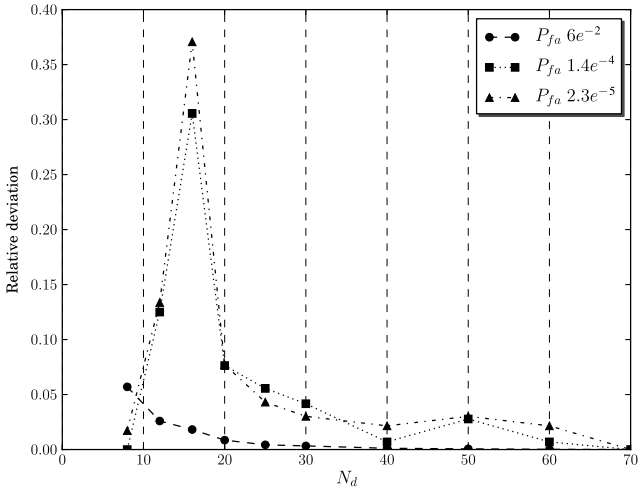

Fig. 12. Relative deviation of P_{fa} for the inner strategy.

linearizations N_d and the strategy influence the probability of failure values. Strategies provide different results which all converge toward the same value, validating the linearization equations. Depending on the requirement, one specific strategy is more interesting than another. Considering a target probability to be reached, the inner polygon strategy provides conservative results for the assembly requirement. In this case, even if the result is an approximation, the probability will not be underestimated. This strategy may be preferred when only one result is expected. On the contrary, for the functional requirement, the conservative results are provided by the outer polygon strategy. Furthermore, the combination of the inner and outer polygon strategies provides a confidence interval for the true failure probability value. The greater the number of linearizations, the smaller the confidence interval. The medium polygon strategy gives the best results, which are very close to the converged value; however these values may not be conservative, which may not be suitable. Yet this strategy may be preferred if a simple approximation of the order of magnitude is required.

5.2.2. Impact of the probability order of magnitude on convergence speed

The previous results concern the impact of the number of linearizations, but the order of magnitude of the target probability can also have an impact. Indeed, the order of magnitude may have an influence on the required number of linearizations to reach a certain accuracy. Figs. 12 and 13 show the relative deviation between the approximate probability and its converged value for the conservative strategy of the assembly and functional requirement. These figures show that the smaller the real probability, the greater the relative deviation. It means that for a given number of linearizations, the relative deviation between the approximated probability and the real probability is greater for a small probability (e.g. 10^{-6}) than for a greater probability (e.g. 10^{-2}). This means that a smaller real probability requires a finer linearization to reach the same accuracy than a greater real probability. In a same way, for a given number of linearizations, the confidence interval of the probability of failure is larger when the real probability is small.

6. Conclusion

The functionality of a product is influenced by design tolerances. Evaluating the quality level of a product at its design stage is therefore a key element, enabling an improvement of the functional quality of the product while reducing the manufacturing cost. This requires methods such as tolerance analysis to quantify the impact of tolerances on mechanism quality. To evaluate the quality level of the product, a mathematical model is required, which must represent its behavior as well as possible. However, the behavior model may be approximated. Therefore the objective

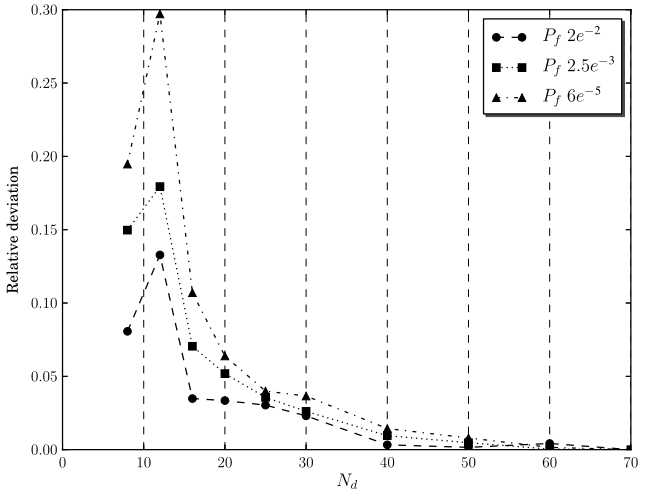

Fig. 13. Relative deviation of P_f for the outer strategy.

of this paper is to answer two questions: "Why is an approximation required?" and "What is its impact on the predicted quality level?".

The paper proposed by Qureshi et al. [1] provides a tolerance analysis formulation able to deal with non-linear behaviors. Although the mathematical formulation enables this kind of problem to be solved, a difficulty appears when calling the optimization scheme with non-linear constraints. Some optimization operations do not converge, making the result unreliable. The present paper is dedicated to defining linearization strategies for the non-linear constraints in order to solve this difficulty. The goal is to demonstrate that applying a linearization procedure has an impact on the predicted quality level (probability of failure). The outcomes of the study are listed below:

- The linearization of non-linear equations is required in both tolerance analysis approaches: tolerance accumulation and displacement accumulation.
- The linearization of non-linear constraints has a real impact on the probability of failure of the mechanism; the obtained result may underestimate the real value, hence over-estimating the quality of the design. The linearization procedure must be chosen carefully in order to obtain conservative results. Indeed, depending on the type of requirement, the conservative strategy is different: inner polygon strategy for the assembly requirement and outer polygon strategy for the functional requirement.
- An interesting procedure consists of defining a confidence interval of the true probability of failure using two linearization strategies: outer and inner polygon. This interval becomes smaller when the number of linearizations increases.
- Approximation due to linearization is all the more important when the real probability of failure is small. This means that the number of linearizations must be greater for a small probability in order to obtain the same accuracy for the results.

Future studies will concern the establishment of a smart algorithm, able to re-use results obtained from a simulation with a poor precision. The idea is that between a simulation with poor precision and one with good precision, a large number of points in the Monte Carlo simulation give the same result. Using the results with poor precision, the goal is to evaluate only those points which may have a different result with a greater degree of linearization. Hence, the computing time to yield an accurate result can be considerably reduced. This algorithm will then be tested on a more complex industrial application.

Acknowledgment

The authors would like to acknowledge the support of ANR "AHTOLA" project (ANR-11- MONU-013).

Appendix A. Behavior model

A.1. Geometrical model

Point A is used as an origin to define the coordinates of the other points:

$$\overrightarrow{AC} = \begin{bmatrix} l_1 \\ l_2 \\ 0 \end{bmatrix} \quad \overrightarrow{AB} = \begin{bmatrix} 0 \\ 0 \\ l_3 \end{bmatrix} \quad \overrightarrow{CD} = \begin{bmatrix} 0 \\ 0 \\ l_4 \end{bmatrix} \quad \overrightarrow{AE} = \begin{bmatrix} 0 \\ 0 \\ -l_5 \end{bmatrix}$$
$$\overrightarrow{CF} = \begin{bmatrix} 0 \\ 0 \\ -l_6 \end{bmatrix} \quad \overrightarrow{AG} = \begin{bmatrix} l_7 \\ l_8 \\ l_9 \end{bmatrix} \quad \overrightarrow{AH} = \begin{bmatrix} l_{10} \\ l_{11} \\ 0 \end{bmatrix}.$$

Deviation torsors $T_{ia/i}$ are defined to model the geometrical deviations of a substitute surface ia with respect to the nominal surface i.

$$\{T_{1b/1}\} = \begin{Bmatrix} a_{1b1} & u_{1b1} \\ b_{1b1} & v_{1b1} \\ 0 & 0 \end{Bmatrix}_A \quad \{T_{2b/2}\} = \begin{Bmatrix} a_{2b2} & u_{2b2} \\ b_{2b2} & v_{2b2} \\ 0 & 0 \end{Bmatrix}_A$$
$$\{T_{1a/1}\} = \begin{Bmatrix} a_{1a1} & 0 \\ b_{1a1} & 0 \\ 0 & w_{1a1} \end{Bmatrix}_A \quad \{T_{2a/2}\} = \begin{Bmatrix} a_{2a2} & 0 \\ b_{2a2} & 0 \\ 0 & w_{2a2} \end{Bmatrix}_A$$
$$\{T_{1c/1}\} = \begin{Bmatrix} a_{1c1} & u_{1c1} \\ b_{1c1} & v_{1c1} \\ 0 & 0 \end{Bmatrix}_C \quad \{T_{2c/2}\} = \begin{Bmatrix} a_{2c2} & u_{2c2} \\ b_{2c2} & v_{2c2} \\ 0 & 0 \end{Bmatrix}_C$$
$$\{T_{1g/1}\} = \begin{Bmatrix} a_{1g1} & u_{1g1} \\ b_{1g1} & v_{1g1} \\ c_{1g1} & w_{1g1} \end{Bmatrix}_G \quad \{T_{2g/2}\} = \begin{Bmatrix} a_{2g2} & u_{2g2} \\ b_{2g2} & v_{2g2} \\ c_{2g2} & w_{2g2} \end{Bmatrix}_G.$$

Other deviations: diameters of the pins and their pin holes: d_{1b}, d_{3b}, d_{1c} and d_{4c}.

Gaps between joints are modeled using clearance torsors:

$$\{G_{1a/2a}\} = \begin{Bmatrix} 0 & U_{1a2a} \\ 0 & V_{1a2a} \\ C_{1a2a} & 0 \end{Bmatrix}_A \quad \{G_{3b/1b}\} = \begin{Bmatrix} a_{3b/1b} & u_{3b/1b} \\ b_{3b/1b} & v_{3b/1b} \\ C_{3b/1b} & W_{3b/1b} \end{Bmatrix}_A$$
$$\{G_{4c/1c}\} = \begin{Bmatrix} a_{4c/1c} & u_{4c/1c} \\ b_{4c/1c} & v_{4c/1c} \\ C_{4c/1c} & W_{4c/1c} \end{Bmatrix}_C \quad \{G_{2g/1g}\} = \begin{Bmatrix} - & u_{2g/1g} \\ - & v_{2g/1g} \\ - & - \end{Bmatrix}_G.$$

A.2. Compatibility equations

Loop (1), (2), (3), expressed in A, gives the following compatibility equations:

$$C_c^{(1)}(\mathbf{X}, \mathbf{G}) = -a_{1b1} - a_{3b1b} + a_{2b2} - a_{2a2} + a_{1a1} = 0 \tag{A.1}$$
$$C_c^{(2)}(\mathbf{X}, \mathbf{G}) = -b_{1b1} - b_{3b1b} + b_{2b2} - b_{2a2} + b_{1a1} = 0 \tag{A.2}$$
$$C_c^{(3)}(\mathbf{X}, \mathbf{G}) = -C_{3b1b} - C_{1a2a} = 0 \tag{A.3}$$
$$C_c^{(4)}(\mathbf{X}, \mathbf{G}) = -u_{1b1} - u_{3b1b} + u_{2b2} - U_{1a2a} = 0 \tag{A.4}$$
$$C_c^{(5)}(\mathbf{X}, \mathbf{G}) = -v_{1b1} - v_{3b1b} + v_{2b2} - V_{1a2a} = 0 \tag{A.5}$$
$$C_c^{(6)}(\mathbf{X}, \mathbf{G}) = -W_{3b1b} - w_{2a2} + w_{1a1} = 0. \tag{A.6}$$

Loop (1), (3), (2), (4), expressed in A, gives the following compatibility equations:

$$C_c^{(7)}(\mathbf{X},\mathbf{G}) = -a_{1b1} - a_{3b1b} + a_{2b2} - a_{2c2} + a_{4c1c} + a_{1c1} = 0 \quad (A.7)$$

$$C_c^{(8)}(\mathbf{X},\mathbf{G}) = -b_{1b1} - b_{3b1b} + b_{2b2} - b_{2c2} + b_{4c1c} + b_{1c1} = 0 \quad (A.8)$$

$$C_c^{(9)}(\mathbf{X},\mathbf{G}) = -C_{3b1b} + C_{4c1c} = 0 \quad (A.9)$$

$$\begin{aligned} C_c^{(10)}(\mathbf{X},\mathbf{G}) &= -u_{1b1} - u_{3b1b} + u_{2b2} - u_{2c2} + u_{4c1c} \\ &\quad + l_2 C_{4c1c} + u_{1c1} = 0 \end{aligned} \quad (A.10)$$

$$\begin{aligned} C_c^{(11)}(\mathbf{X},\mathbf{G}) &= -v_{1b1} - v_{3b1b} + v_{2b2} - v_{2c2} \\ &\quad + v_{4c1c} - l_1 C_{4c1c} + v_{1c1} = 0 \end{aligned} \quad (A.11)$$

$$\begin{aligned} C_c^{(12)}(\mathbf{X},\mathbf{G}) &= -W_{3b1b} - l_1 b_{2c2} + l_2 a_{2c2} + W_{4c1c} \\ &\quad + l_1 b_{4c1c} - l_2 a_{4c1c} + l_1 b_{1c1} - l_2 a_{1c1} = 0. \end{aligned} \quad (A.12)$$

A.3. Functional condition

The functional characteristic is given by:

$$\begin{aligned} u_{2g1g} + v_{2g/1g} &= u_{1b1} + l_9 b_{1b1} + u_{3b1b} - l_8 C_{3b1b} \\ &\quad + l_9 b_{3b1b} - u_{2b2} - l_9 b_{2b2} + u_{2g2} - u_{1g1} \\ &\quad + v_{1b1} - l_9 a_{1b1} + v_{3b1b} - l_9 a_{3b1b} \\ &\quad + l_7 C_{3b1b} - v_{2b2} + l_9 a_{2b2} + v_{2g2} - v_{1g1}. \end{aligned} \quad (A.13)$$

This characteristic must not exceed a threshold d_{th}. The functional condition is given as follows:

$$C_f(\mathbf{X},\mathbf{G}) = d_{th} - (u_{2g1g} + v_{2g/1g}) \geq 0. \quad (A.14)$$

A.4. Interface constraints

The non-interference conditions concern both pins.

Non-interference $1b/3b$:

$$C_i^{(1)} = u_{3b1b}^2 + v_{3b1b}^2 - \left(\frac{d_{1b} - d_{3b}}{2}\right)^2 \leq 0 \quad (A.15)$$

$$\begin{aligned} C_i^{(2)} &= (u_{3b1b} + l_3 b_{3b1b})^2 + (v_{3b1b} - l_3 a_{3b1b})^2 \\ &\quad - \left(\frac{d_{1b} - d_{3b}}{2}\right)^2 \leq 0. \end{aligned} \quad (A.16)$$

Non-interference $1c/4c$:

$$C_i^{(3)} = u_{4c1c}^2 + v_{4c1c}^2 - \left(\frac{d_{1c} - d_{4c}}{2}\right)^2 \leq 0 \quad (A.17)$$

$$\begin{aligned} C_i^{(4)} &= (u_{4c1c} + l_4 b_{4c1c})^2 + (v_{4c1c} - l_4 a_{4c1c})^2 \\ &\quad - \left(\frac{d_{1c} - d_{4c}}{2}\right)^2 \leq 0. \end{aligned} \quad (A.18)$$

A.5. Deviation rotation relations

Rotation deviation expressions for deviation torsors are given as follows:

- **Torsor** $\{T_{1a/1}\}$:

$$\begin{aligned} a_{1a1} &= \frac{l_1}{l_1 l_{11} - l_2 l_{10}} w_{1a1,H} + \frac{l_{10} - l_1}{l_1 l_{11} - l_2 l_{10}} w_{1a1} \\ &\quad - \frac{l_{10}}{l_1 l_{11} - l_2 l_{10}} w_{1a1,C} \end{aligned} \quad (A.19)$$

$$\begin{aligned} b_{1a1} &= \frac{l_2}{l_1 l_{11} - l_2 l_{10}} w_{1a1,H} + \frac{l_{11} - l_2}{l_1 l_{11} - l_2 l_{10}} w_{1a1} \\ &\quad - \frac{l_{11}}{l_1 l_{11} - l_2 l_{10}} w_{1a1,C}. \end{aligned} \quad (A.20)$$

- **Torsor** $\{T_{2a/2}\}$:

$$\begin{aligned} a_{2a2} &= \frac{l_1}{l_1 l_{11} - l_2 l_{10}} w_{2a2,H} + \frac{l_{10} - l_1}{l_1 l_{11} - l_2 l_{10}} w_{2a2} \\ &\quad - \frac{l_{10}}{l_1 l_{11} - l_2 l_{10}} w_{2a2,C} \end{aligned} \quad (A.21)$$

$$\begin{aligned} b_{2a2} &= \frac{l_2}{l_1 l_{11} - l_2 l_{10}} w_{2a2,H} + \frac{l_{11} - l_2}{l_1 l_{11} - l_2 l_{10}} w_{2a2} \\ &\quad - \frac{l_{11}}{l_1 l_{11} - l_2 l_{10}} w_{2a2,C}. \end{aligned} \quad (A.22)$$

- **Torsor** $\{T_{1b/1}\}$:

$$a_{1b1} = \frac{v_{1b1} - v_{1b1,B}}{l_3} \quad (A.23)$$

$$b_{1b1} = \frac{u_{1b1,B} - u_{1b1}}{l_3}. \quad (A.24)$$

- **Torsor** $\{T_{2b/2}\}$:

$$a_{2b2} = \frac{-v_{2b2} + v_{2b2,E}}{l_5} \quad (A.25)$$

$$b_{2b2} = \frac{-u_{2b2,E} + u_{2b2}}{l_5}. \quad (A.26)$$

- **Torsor** $\{T_{1c/1}\}$:

$$a_{1c1} = \frac{v_{1c1} - v_{1c1,D}}{l_4} \quad (A.27)$$

$$b_{1c1} = \frac{u_{1c1,D} - u_{1c1}}{l_4}. \quad (A.28)$$

- **Torsor** $\{T_{2c/2}\}$:

$$a_{2c2} = \frac{-v_{2c2} + v_{2c2,F}}{l_6} \quad (A.29)$$

$$b_{2c2} = \frac{-u_{2c2,F} + u_{2c2}}{l_6}. \quad (A.30)$$

Appendix B. Parameter values

Nominal values for the three set of values:

l_1	l_2	l_3	l_4	l_5	l_6	l_7	l_8	l_9	l_{10}	l_{11}
100	40	30	30	20	20	120	50	40	50	−30

Threshold values:

	y_{th}		
Set of values	1	2	3
	0.25	0.25	0.28

Random variables:

	μ_X	σ_X		
Set of values	All	1	2	3
d_{1b}	20	0.06	0.01	0.01
d_{3b}	19.8	0.06	0.01	0.01
d_{1c}	20	0.06	0.01	0.01
d_{4c}	19.8	0.06	0.01	0.01
t	0	0.01	0.01	0.009
r	0	0.01	0.01	0.0009

where t is the vector of the translation components of the geometrical deviations:

$$\begin{aligned} t = \{&u_{1b1}, v_{1b1}, u_{1b1,B}, v_{1b1,B}, u_{2b2}, v_{2b2}, u_{2b2,E}, v_{2b2,E}, w_{1a1}, \\ &w_{1a1,H}, w_{1a1,C}, w_{2a2}, w_{2a2,H}, w_{2a2,C}, u_{1c1}, v_{1c1}, u_{1c1,D}, \\ &v_{1c1,D}, u_{2c2}, v_{2c2}, u_{2c2,F}, v_{2c2,F}, \\ &u_{1g1}, v_{1g1}, w_{1g1}, u_{2g2}, v_{2g2}, w_{2g2}\} \end{aligned}$$

Table C.4
Probabilities of failure obtained with the second set of values.

	Set of values 2					
	P_{fa} ($\times 10^{-4}$)			P_f ($\times 10^{-3}$)		
$N_{samples}$	3e6			3e6		
C.O.V.	∼4.8%			∼1.15%		
95% C.I.	∼0.27			∼0.12		
N_d	Inner	Medium	Outer	Inner	Medium	Outer
8	1.44	0.71	0.42	1.28	1.93	2.9
12	1.62	1.22	0.91	2.07	2.49	2.98
16	1.88	1.62	1.36	2.21	2.45	2.7
20	1.55	1.37	1.26	2.33	2.48	2.66
25	1.52	1.43	1.36	2.41	2.5	2.62
30	1.5	1.42	1.35	2.45	2.52	2.59
40	1.43	1.38	1.36	2.47	2.51	2.55
50	1.48	1.45	1.42	2.49	2.52	2.54
60	1.43	1.42	1.4	2.49	2.51	2.53
70	1.44	1.42	1.42	2.5	2.52	2.52

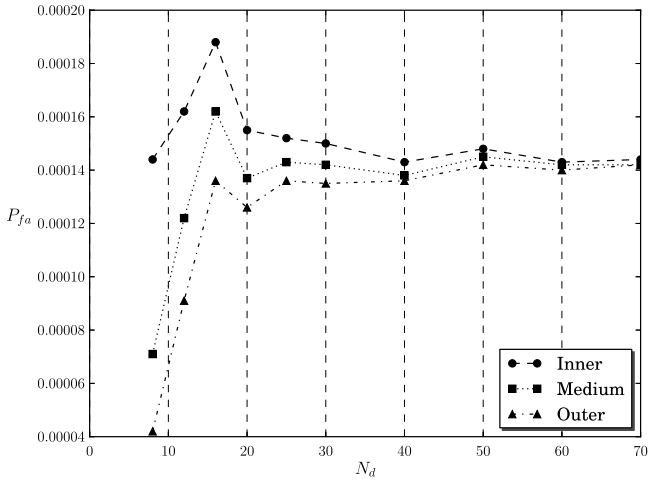

Fig. C.14. Convergence of the probability of failure of the assembly requirement for the second set of values.

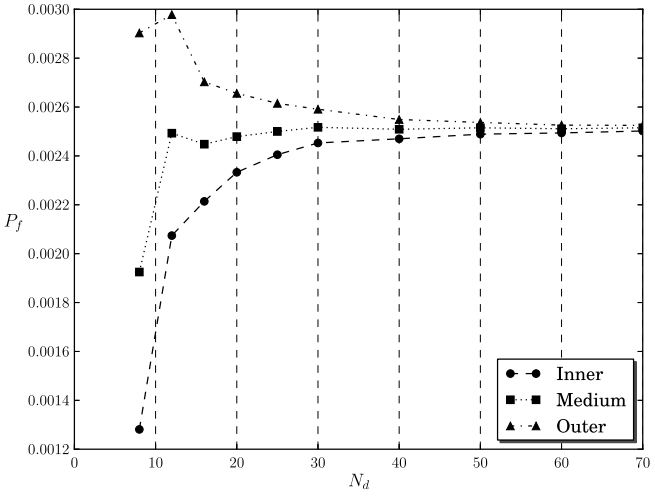

Fig. C.15. Convergence of the probability of failure of the functional requirement for the second set of values.

and r is the vector of the rotation components of the geometrical deviations:

$r = \{a_{1g1}, b_{1g1}, c_{1g1}, a_{2g2}, b_{2g2}, c_{2g2}\}$.

Appendix C. Results for the second set of values

See Table C.4, Figs. C.14 and C.15.

Table D.5
Probabilities of failure obtained with the third set of values.

	Set of values 3					
	P_{fa} ($\times 10^{-5}$)			P_f ($\times 10^{-5}$)		
$N_{samples}$	1e7			1e7		
C.O.V.	∼6%			∼4%		
95% C.I.	∼0.6			∼0.1		
N_d	Inner	Medium	Outer	Inner	Medium	Outer
8	2.28	1.07	0.47	2.26	4.10	7.48
12	2.63	1.98	1.32	4.65	6.16	8.12
16	3.18	2.63	2.20	4.98	5.87	6.93
20	2.50	2.25	2.05	5.44	6.09	6.66
25	2.42	2.35	2.16	5.81	6.18	6.51
30	2.39	2.24	2.19	5.98	6.23	6.49
40	2.27	2.24	2.19	6.04	6.18	6.35
50	2.39	2.33	2.27	6.13	6.21	6.31
60	2.27	2.24	2.24	6.12	6.19	6.27
70	2.32	2.27	2.24	6.17	6.20	6.26

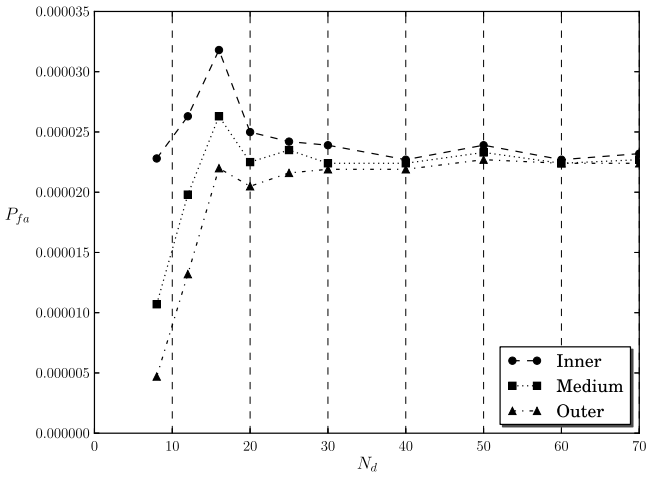

Fig. D.16. Convergence of the probability of failure of the assembly requirement for the third set of values.

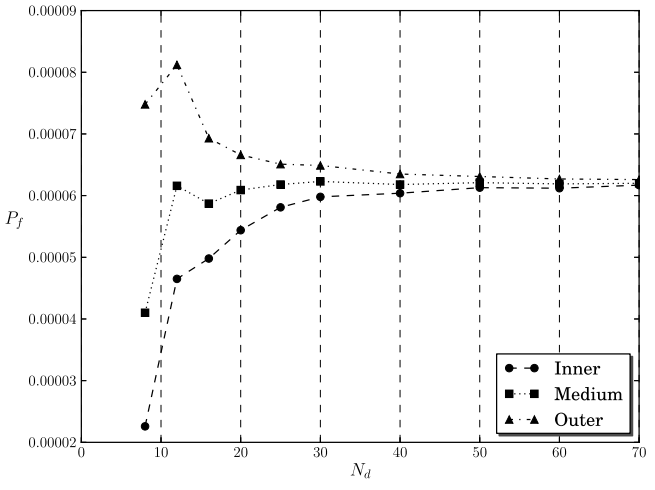

Fig. D.17. Convergence of the probability of failure of the functional requirement for the third set of values.

Appendix D. Results for the third set of values

See Table D.5, Figs. D.16 and D.17.

References

[1] Qureshi A, Dantan J, Sabri V, Beaucaire P, Gayton N. A statistical tolerance analysis approach for over-constrained mechanism based on optimization

and monte carlo simulation. Comput Aided Des 2012;44:132–42 http://dx.doi.org/10.1016/j.cad.2011.10.004.
[2] Dantan J, Qureshi A. Worse case and statistical tolerance analysis based on quantified constraint satisfaction problems and monte carlo simulation. Comput Aided Des 2009;41(1):1–12. http://dx.doi.org/10.1016/j.cad.2008.11.003.
[3] Dantan J, Gayton N, Dumas A, Etienne A, Qureshi A. Mathematical issues in mechanical tolerance analysis, presented at: 13th Colloque National AIP Priméca, Le Mont–Dore. 2012, pp. 12p.
[4] Desrochers A. Geometrical variations management in a multidisciplinary environment with the Jacobian–Torsor model. In: Davidson JK, editor. Models for computer aided tolerancing in design and manufacturing. 2007. p. 75–84. http://dx.doi.org/10.1007/1-4020-5438-6_9.
[5] Loose J, Zhou S, Ceglarek D. Kinematic analysis of dimensional variation propagation for multistage machining processes with general fixture layouts. IEEE Trans Autom Sci Eng 2007;4:141–52 http://dx.doi.org/10.1109/TASE.2006.877393.
[6] Bourdet P, Clément A. Controlling a complex surface with a 3 axis measuring machine. Annal CIRP 1976;25:359–64.
[7] Legoff O, Tichadou S, Hascoet J. Manufacturing errors modelling: two three-dimensional approaches. Proc Inst Mech Eng B 2004;218:1869–73 http://dx.doi.org/10.1177/095440540421801219.
[8] Chase K, Magleby S, Glancy C. Tolerance analysis of 2-D and 3-D mechanical assemblies with small kinematic adjustments. In: Zhang HC, editor. Advanced tolerancing techniques, vol. 218. Wiley; 2004. p. 1869–73.
[9] Gao J, Chase K, Magleby S. Generalized 3-d tolerance analysis of mechanical assemblies with small kinematic adjustments. IIE Trans 1998;30:367–77. http://dx.doi.org/10.1023/A:1007451225222.
[10] Bhide S, Ameta G, Davidson J, Shah J. Tolerance-maps applied to the straightness and orientation of an axis, In: CD ROM Proc., 9th CIRP international seminar on computer-aided tolerancing, Arizona State University, http://dx.doi.org/10.1007/1-4020-5438-6_6.
[11] Davidson J, Shah J. Modeling of geometric variations for line-profiles. J Comput Inf Sci Eng 2012;12:1–10. http://dx.doi.org/10.1115/1.4007404.
[12] Giordan M, Duret D. Clearance space and deviation space: application to three-dimensional chain of dimensions and positions. In: 3rd CIRP design seminar on computer-aided tolerancing.
[13] Giordano M, Samper S, Petit J. Tolerance analysis and synthesis by means of deviation domains, axi-symmetric cases. In: 9th CIRP international seminar on computer-aided tolerancing, Arizona State University, http://dx.doi.org/10.1007/1-4020-5438-6_10.
[14] Nigam S, Turner J. Review of statistical approaches of tolerance analysis. Comput Aided Des 1995;27:6–15 http://dx.doi.org/10.1016/0010-4485(95)90748-5.
[15] Ballu A, Plantec J-Y, Mathieu L. Geometrical reliability of overconstrained mechanisms with gaps. CIRP Ann Manuf Technol 2009;57:159–62 http://dx.doi.org/10.1016/j.cirp.2008.03.038.
[16] Mhenni F, Serré P, Mlika A, Romdhane L, Rivière A. Dependency between dimensional deviations in overconstrained mechanisms. Conception et Production intégrées (Rabat, Maroc, October 2007) p. 22–4.
[17] Davidson J, Mujezinovic A, Shah J. A new mathematical model for geometric tolerances as applied to round faces. J Mech Des 2002;124:609–22 http://dx.doi.org/10.1115/1.1497362.
[18] Zou Z, Morse E. Applications of the gapspace model for multidimensional mechanical assemblies. J Comput Inf Sci Eng 2003;12:22–30. http://dx.doi.org/10.1115/1.1565072.
[19] Morse E. Statistical analysis of assemblies having dependent fitting conditions, In: ASME (Ed.), International mechanical engineering congress and exposition. 2004, p. 1–5. http://dx.doi.org/10.1115/IMECE2004-61664.
[20] Ameta G, Samper S, Giordano M. Comparison of spatial math models for tolerance analysis: tolerance-maps, deviation domain, and TTRS. J Comput Inf Sci Eng 2012;12:1–10. http://dx.doi.org/10.1115/1.3593413.
[21] Ameta G, Davidson J, Shah J. Effects of size, orientation, and form tolerances on the frequency distributions of clearance between two planar faces. J Comput Inf Sci Eng 2011;11:1–10. http://dx.doi.org/10.1115/1.3503881.
[22] Samper S, Adragna P-A, Favreliere H, Pairel E, Hernandez P. Rigid and elastic precision domains of ball bearings. J Comput Inf Sci Eng 2012;12:1–13. http://dx.doi.org/10.1115/1.3615686.
[23] Mansuy M, Giordano M, Hernandez P. A generic method for the worst case and statistical tridimensional tolerancing analysis, In: Elsevier (Ed.), Procedia Engineering, 2012, pp. 10p, presented at: 12th CIRP International seminar on computer–aided tolerancing, http://dx.doi.org/10.1016/j.procir.2013.08.042.
[24] Beaucaire P, Gayton N, Duc E, Dantan J-Y. Statistical tolerance analysis of over-constrained mechanisms with gaps using system reliability methods. Comput-Aided Des 2013;45:1547–55. http://dx.doi.org/10.1016/j.cad.2011.10.004.
[25] Hong Y, Chang T. A comprehensive review of tolerancing research. Int J Prod Res 2002;40:2425–59. http://dx.doi.org/10.1080/00207540210128242.
[26] Mansuy M, Giordano M, Hernandez P. A new calculation method for the worst case tolerance analysis and synthesis in stack-type assemblies. Comput-Aided Des 2011;43:1118–25. http://dx.doi.org/10.1016/j.cad.2011.04.010.